Nanoscale Res Lett (2007) 2:12–16
DOI 10.1007/s11671-006-9022-8

NANO EXPRESS

Nanocrystal and surface alloy properties of bimetallic Gold-Platinum nanoparticles

Derrick Mott · Jin Luo · Andrew Smith · Peter N. Njoki · Lingyan Wang · Chuan-Jian Zhong

Published online: 30 November 2006

Abstract We report on the correlation between the nanocrystal and surface alloy properties with the bimetallic composition of gold-platinum(AuPt) nanoparticles. The fundamental understanding of whether the AuPt nanocrystal core is alloyed or phase-segregated and how the surface binding properties are correlated with the nanoscale bimetallic properties is important not only for the exploitation of catalytic activity of the nanoscale bimetallic catalysts, but also to the general exploration of the surface or interfacial reactivities of bimetallic or multimetallic nanoparticles. The AuPt nanoparticles are shown to exhibit not only single-phase alloy character in the nanocrystal, but also bimetallic alloy property on the surface. The nanocrystal and surface alloy properties are directly correlated with the bimetallic composition. The FTIR probing of CO adsorption on the bimetallic nanoparticles supported on silica reveals that the surface binding sites are dependent on the bimetallic composition. The analysis of this dependence further led to the conclusion that the relative Au-atop and Pt-atop sites for the linear CO adsorption on the nanoparticle surface are not only correlated with the bimetallic composition, but also with the electronic effect as a result of the d-band shift of Pt in the bimetallic nanocrystals, which is the first demonstration of the nanoscale core-surface property correlation for the bimetallic nanoparticles over a wide range of bimetallic composition.

Keywords Gold-Platinum nanoparticles · Nanocrystal alloy · Surface binding sites · Bimetallic composition

Materials at nanoscale dimension often display unique chemical properties not found in the bulk counterparts [1]. The key to exploring such properties is the ability to control size, composition, and surface binding properties of the nanomaterials [1, 2]. Gold-based nanoparticles present an intriguing system for delineating the correlation between the chemical properties and the nanoscale control properties. Despite the intensive research into the catalytic activity of Au in a restricted nanoscale size range [3], the catalytic origin of nanosized gold and Au-based bimetallic catalysts remain elusive. One of the main problems is the lack of understanding of the nanoscale core-surface property correlation. In this report, Au-Pt nanoparticles of 2~4 nm diameter are investigated to address some of the fundamental questions on the nanoscale phase and surface binding properties in view of the recent ability to synthesize Au-Pt nanoparticles with a wide range of bimetallic composition [4]. There are two fundamental questions: (1) is the Au-Pt nanocrystal core alloy or phase-segregated? (2) how are the surface binding properties correlated with the nanoscale bimetallic properties? The answers to these questions have important implications not only to the exploitation of catalytic activity of the nanoscale bimetallic catalysts, but also to the general exploration of the surface or

Electronic Supplementary Material Supplementary material is available to authorised users in the online version of this article at http://dx.doi.org/10.1007/s11671-006-9022-8

D. Mott · J. Luo · A. Smith · P. N. Njoki · L. Wang · C.-J. Zhong (✉)
Department of Chemistry, State University of New York at Binghamton, Binghamton, New York 13902, USA
e-mail: cjzhong@binghamton.edu

interfacial reactivities of bimetallic or multimetallic nanoparticles. For the nanocrystal core, our recent XRD data [4a] revealed the presence of unique alloy properties that are in sharp contrast to the miscibility gap known for the bulk counterpart [4b]. For the nanocrystal surface, while there are theoretical simulation approaches to predicting surface segregation [1], many experimental surface techniques such as XPS could not provide adequate information because the depth sensitivity is larger than the particle size. HRTEM cannot conclusively address the surface properties either because the surface of the nanocrystal of this size region is populated with corners and edges. In contrast, an infrared spectroscopic study of CO probe on the nanoparticles can effectively address fundamental issues related to the surface binding properties because its streching frequency is highly sensitive to the surface binding sites [5], as widely reported for oxide-supported gold, platinum, gold-platinum and other bimetallic catalysts prepared by vapor deposition [6], cation-exchange, insipient wetness impregnation [7], and dendrimer or cluster based methods [7, 8]. We report herein the findings of an investigation of the nanoscale core and surface properties of Au-Pt nanoparticles of different bimetallic composition. The results provide new and important insights into the correlation between the nanoscale core and surface properties over a wide range of bimetallic composition [9, 10].

The Au-Pt catalysts were prepared by a combination of two protocols. The first involved a modified two-phase synthesis [11] of nanoparticles of ~2 nm core sizes with different compositions (Au_mPt_{100-m}) capped with a mixed monolayer of decanethiolate and oleylamine [12, 13]. The second involved assembly of the as-synthesized nanoparticles on silica [10] followed by subsequent thermal treatment under controlled temperature and atmosphere [9]. The actual loading ranged from 2.5 to 5.4% by mass for typical samples. The silica-loaded nanoparticles were thermally-treated under controlled atmosphere and temperature, including shell removal under 300 °C with 20% O_2/N_2 for 1 hour and calcination under 400°C with 15% H_2/N_2 for 2 h. The average sizes of the as-synthesized particles determined from TEM data are 2.2 ± 0.2 nm for Au, 4.8 ± 0.8 nm for Pt, and 1.8 ± 0.6 nm for $Au_{82}Pt_{18}$ nanoparticles. While the average sizes were slightly increased (e.g., 3.8 ± 0.7 nm for Au/SiO_2 and 3.3 ± 0.4 for $Au_{82}Pt_{18}/SiO_2$) in comparison with the as-synthesized particles, they displayed high monodispersity.

The bimetallic composition was analyzed by direct current plasma - atomic emission spectroscopy (DCP-AES (ARL Fisons SS-7)), which involved dissolving the nanoparticles in aqua regia solution for sample preparation [4a]. Powder X-ray diffraction data were collected on a Philips X'Pert and a Scintag XDS 2000 diffractometers using Cu Kα radiation (λ = 1.5418 Å). The composition was also estimated by analyzing the XRD data for the bimetallic catalysts of different composition, which involved fitting the values of the lattice parameters [4a]. The sample cell for the FTIR measurement consists of two valves in the glass tube, which allowed for purging with nitrogen and CO. The thermally-treated catalysts were ground into fine powders and pressed into a pellet, which was mounted in a glass tube enclosed in a metal sheath with NaCl window plates at each end (a gas-tight environment) for the transmission FTIR measurement. Sixty four scans were collected for each spectrum with a resolution of 4 cm^{-1}. Spectra were acquired at room temperature by first purging the chamber with nitrogen and then taking a background spectrum. The chamber was then purged with ~4% CO in nitrogen (for 10 min), and a spectrum was taken. By subtracting the spectrum of the gas-phase CO (2171 and 2119 cm^{-1}) generated in a separate measurement under the same conditions without the catalyst, the resulting spectrum was obtained that corresponded to the CO molecules adsorbed on the catalyst. All spectra were baseline corrected and water subtracted.

An examination of the XRD data for AuPt nanoparticles over a wide range of bimetallic composition, part of which was recently reported [4a], provides important information for assessing the phase properties of the bimetallic nanomaterials. The control of AuPt composition in the range of 10–90%Au with 2–4 nm core sizes and high monodispersity (< ±0.5 nm) was achieved by manipulating the precursor feed ratio. The Au_mPt_{100-m} nanoparticles were readily assembled on different supports (e.g., carbon (C) and silica (SiO_2)) and underwent thermal treatment. Figure 1 shows the lattice parameters as a function of bimetallic composition comparing both bulk and nanoscale AuPt systems. The open circles correspond to data for bulk bimetallic metal system, whereas the open triangle points correspond to frozen states of bulk bimetallic metal system. For the bimetallic nanoparticles, the half-filled circle points correspond to data vs. bimetallic composition determined from analyzing the values of the lattice parameter for the bimetallic nanoparticles [4a], whereas filled circle points correspond to data vs. bimetallic composition determined from DCP-AES analysis of the bimetallic nanoparticles. In contrast to the bulk Au-Pt counterpart which display a miscibility gap at 20~ 90%Au [4b], as shown by the blue data points and lines in Figure 1, the lattice parameters of the bimetallic nanoparticles, as shown by the red and pink data points and lines in Figure 1, were found to

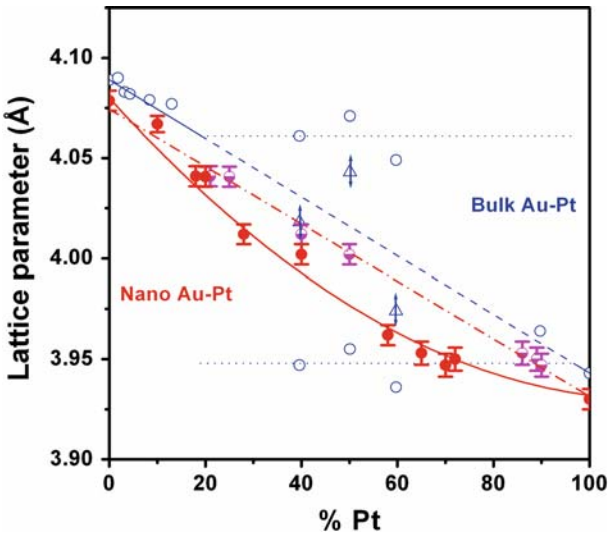

Fig. 1 The lattice parameters vs. Pt% for AuPt nanoparticles (the red and pink data points and lines), part of the data reported recently [4a], and for bulk AuPt [4b] (the open circle data points and lines (blue)). For bulk AuPt, the triangle points (blue) represent those at frozen states. For nanoscale AuPt, the half-filled circle points (pink) represent those using the composition derived from fitting the lattice parameter from XRD data, whereas the filled circled points (red) represent those using the composition derived from DCP analysis

exhibit either linear or slightly-curved relationships with Pt%. The linear relationship follows a Vegard's type law typically observed with binary metallic alloys. The difference between the linear (pink data points) and the slightly-curved (red data points) relationships reflects the limitation of the composition determination using data from the XRD analysis and the DCP-AES analysis. The former is an indirect estimate of the composition. The latter is a direct determination, which could however be affected by the presence of a small fraction of physically-mixed Au and Pt nanoparticles in the bimetallic AuPt sample. While a more precise measurement of the bimetallic composition is needed (e.g., using high resolution TEM-EDX method), we believe that the likely lattice parameter-composition correlation should fall in between the linear and the slightly-curved features. Nevertheless, this finding demonstrates the alloy properties for the bimetallic AuPt nanoparticles.

In addition, the fact that the lattice parameter values of the nanoscale AuPt are all smaller than those for the bulk AuPt is an intriguing phenomenon, which suggests that nanoparticles have smaller inter-atomic distances than those for the bulk counterparts. To our knowledge, this is the first example demonstrating that the nanoscale AuPt nanoparticles not only have single-phase character but also small inter-atomic distances in the entire bimetallic composition range, both of which are in sharp contrast to those known for their bulk counterparts.

A comparison among infrared spectra for CO adsorption on AuPt nanoparticles over a wide range of bimetallic composition provides important information for assessing the surface binding properties of the bimetallic nanomaterials. By comparing CO spectra for Au/SiO_2, Pt/SiO_2, physical mixtures of Au/SiO_2 and Pt/SiO_2, and an $Au_{72}Pt_{28}/SiO_2$ alloy (see supporting information), the CO bands for the bimetallic alloy catalyst are detected at 2115 cm^{-1} and 2066 cm^{-1}, which are distinctively different from the single band feature at 2115 cm^{-1} for CO linearly adsorbed on atop sites of Au [2, 5, 14, 15], and the single band feature at 2096 cm^{-1} for CO on atop sites for Pt [5]. The general feature is in agreement with observations reported in two previous studies [7, 8] for gold-platinum bimetallic catalysts synthesized by other methods. For example, for AuPt prepared by a 1:1-feeding ratio in a dendrimer-based synthesis [8], the observed 2113 cm^{-1} band was attributed to adsorption on Au sites though the band for CO on monometallic gold was not detected, and a 2063-cm^{-1} band was attributed to CO on Pt sites which was explained due to dilution and dipole coupling effects. For the cluster-derived AuPt bimetallic catalyst [7], the observed 2117 cm^{-1} band was similarly attributed to CO adsorbed to Au sites and the observed 2064 cm^{-1} band was assigned to CO at Pt sites due to an electronic effect caused by the incorporation of Au to the bimetallic catalyst and not the dipolar coupling effect as supported by ^{13}CO data.

To correlate the CO bands with the bimetallic composition, it is essential to prepare the nanomaterials in a wide range of bimetallic composition. Our ability to prepare AuPt nanoparticles in a wide range of bimetallic composition, which were already proven by XRD to display single-phase alloy properties [4], allowed us to probe the surface-composition correlation. Figure 2 shows a representative set of FTIR spectra comparing CO adsorption on $AuPt/SiO_2$ with a wide range of bimetallic compositions.

Two most important features can be observed from the spectral evolution as a function of bimetallic composition. First, the 2115-cm^{-1} band observed for Au/SiO_2 (a) displays a clear trend of diminishing absorbance as Pt concentration increases in the bimetallic catalysts. It is very interesting that this band becomes insignificant or even absent at > ~45% Pt. Secondly, the lower-frequency CO band (~2050 cm^{-1}) shows a clear trend in shift towards that for the Pt-atop CO band observed for Pt/SiO_2 (i) as Pt concentration increases. This trend is shown in Figure 3. For higher concentrations of Au, this band is strong and broad.

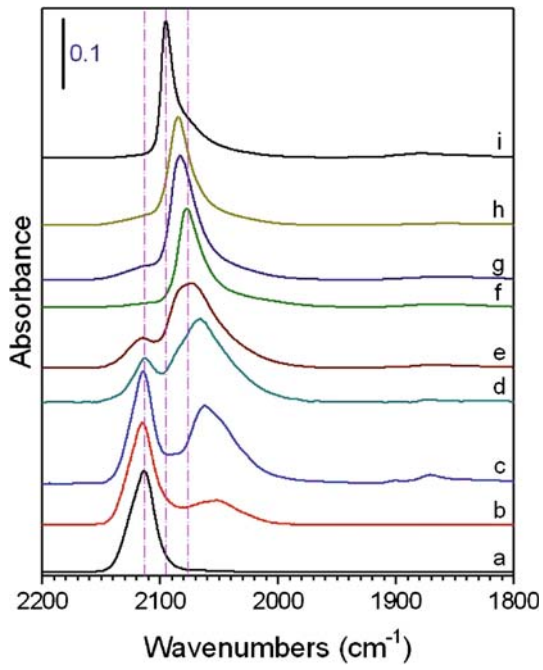

Fig. 2 Comparison of FTIR spectra of CO adsorption: (a) Au/SiO_2, (b) $Au_{96}Pt_4/SiO_2$, (c) $Au_{82}Pt_{18}/SiO_2$, (d) $Au_{72}Pt_{28}/SiO_2$, (e) $Au_{65}Pt_{35}/SiO_2$, (f) $Au_{56}Pt_{44}/SiO_2$, (g) $Au_{43}Pt_{57}/SiO_2$, (h) $Au_{35}Pt_{65}/SiO_2$, and (i) Pt/SiO_2

Such a dependence of the CO bands on the bimetallic concentration is remarkable, and is to our knowledge observed for the first time. The higher-frequency band

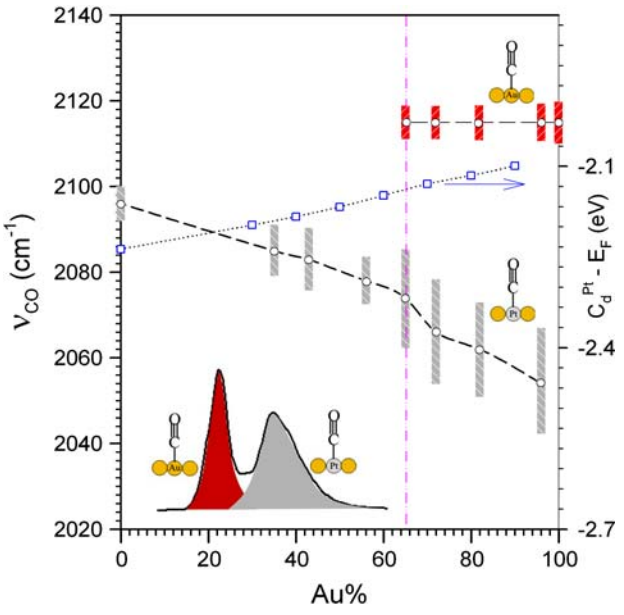

Fig. 3 Plot of the frequency for Au-atop and Pt-atop CO bands vs the composition of Au in the alloy AuPt nanoparticles. The length of the bars represents half of the peak width (determined from the full width at half of the peak maximum). The dotted line with squares represents the average d-band shift for Pt atoms based on calculation results in ref-16

(2115 cm^{-1}) is attributed to CO adsorption on Au-atop sites in a Au-rich surface environment, whereas the lower-frequency band and its composition-dependent shift reflect an electronic effect of the surface Pt-atop sites alloyed in the bimetallic nanocrystal. The fact that the disappearance of the Au-atop CO band at > ~45% Pt is accompanied by a gradual shift of the Pt-atop CO band is indicative of a unique synergistic surface property in which the Pt-atop CO adsorption is greatly favoured over the Au-atop CO adsorption. To understand this preference, we must understand how Au atoms surrounding Pt atoms produce an electronic effect on the binding properties of CO on Pt.

The understanding of the electronic effect is based on the correlation between the spectral features and findings from a previous density functional theory (DFT) calculation on the d-band of Pt atoms in bimetallic AuPt surfaces [16]. The DFT calculation showed that the d-band center of Pt atoms increases with Au concentration in the AuPt alloy on a Au(111) or Pt(111) substrate. For an AuPt alloy on Au(111), the d-band center of Pt atoms was found to show an increase from 0 to 65~70% Au, after which a slight decrease was observed. For a AuPt alloy on Pt(111), the d-band center of Pt atoms is found to increase almost linearly with the concentration of Au. Both were supported by experimental data in which the adsorption of CO showed an increased binding energy in comparison with Pt(111), due to the larger lattice constant of Au, leading to an expansion of Pt [16, 17]. The average d-band shift for Pt atoms from these two sets of DFT calculation results is included in Figure 3 to illustrate the general trend. To aid the visualization of the finding, Scheme 1 depicts surface atomic distribution on an idealized bimetallic nanocrystal, on which a homogeneous distribution of Pt atoms in Au atoms is assumed based on the single-phase alloy nature [8].

Since the DFT results provide information on the Pt surface binding properties, let us consider the maximum concentration of Pt atoms on a surface in which each Pt atom is completely surrounded by Au atoms. The Pt concentration is 33% for $\sqrt{3} \times \sqrt{3}R30^0$ (111) or 50% for 2×2 (100) for a single layer bimetallic surface, and 25% (111) or 16% (100) for a multi-layer structure. An average of these values would yield 30~ 33%, which coincides closely with the observed maximum of the d-band for Pt atoms in an AuPt alloy on Au(111) [16]. Interestingly, a subtle transition for the lower-frequency band, i.e., from a relatively-broad band feature to a narrow band feature that resembles that of the Pt-atop CO band (Figure 2), is observed to occur at ~ 65% Au, below which the Au-atop CO band basically disappeared. There exists a stronger electron donation to the

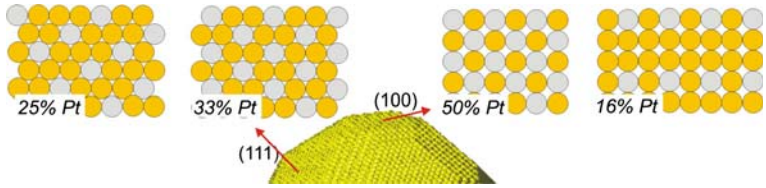

Scheme 1 Distribution of Pt (grey) in Au atoms (orange) on the surfaces of an idealized bimetallic nanocrystal

CO band by a Pt-atop site surrounded by Au atoms in the bimetallic alloy surface than that from the monometallic Pt surface as a consequence of the upshift in d-band center of Pt atoms surrounded by Au atoms (Figure 2), which explains the preference of Pt-atop CO over the Au-atop CO adsorption. The observed decrease of the Pt-atop CO band frequency with increasing Au concentration is clearly in agreement with the d-band theory for the bimetallic system [16]. Note that the observed frequency region of 2050 – 2080 cm^{-1} is quite close to those found recently based on DFT calculations of CO adsorption on AuPt clusters (2030 and 2070 cm^{-1}) depending on the binding site (Pt or Au) [18, 19].

It is important to note that the complete disappearance of the Au-CO band for samples with a concentration below 65% Au does not necessarily imply the absence of Au on the surface of the nanoparticles; it implies rather the preferential Pt-atop CO adsorption over Au-atop CO adsorption, which is supported by the DFT calculation results [16]. This is an important finding in contrast to the linear lattice parameter for the bimetallic alloy nanoparticles of different composition evidenced by recent XRD data [4a]. In this regard, the results form both XPS and HRTEM analyses could not provide such information due to the depth profile of XPS being larger than the particle sizes and the high population of corner or edge atoms on the nanocrystal surface. We also note that our assessment of the surface bimetallic properties is in fact supported by electrochemical measurements. For example, the detection of redox waves corresponding to Au and Pt for AuPt alloy nanoparticles of different bimetallic composition on electrode surfaces demonstrated the presence of the bimetallic surface composition consistent with the bimetallic nanoparticle core composition determined experimentally (see Supporting Information).

In conclusion, we have shown that the AuPt nanoparticles exhibit bimetallic surface properties. This finding further led to the correlation of the Au-atop and Pt-atop CO bands on the surface of the alloy nanoparticles of a wide range of bimetallic composition with the electronic effect as a result of the d-band shift of Pt in the bimetallic nanocrystals. This finding, together with the previous findings of the nanocrystal core properties [4a], has provided the first evidence that both the core and the surface of Au-Pt nanoparticles exhibit bimetallic alloy properties. Further quantitative correlation of the findings with theoretical modeling based on density functional theory [1, 16, 18, 19] along with studies of the catalytic or interfacial reactivities, will provide mechanistic details into fundamental questions related to the bimetallic nanoparticles and catalysts.

Acknowledgments This work was supported in part by the National Science Foundation (CHE 0316322), the Petroleum Research Fund administered by the American Chemical Society (40253-AC5M), and the GROW Program of World Gold Council. We also thank Dr. H. R. Naslund for DCP-AES analysis, and Dr. V. Petkov for XRD analysis.

References

1. G.F. Wang, M.A.Van Hove, P.N. Ross, M.I. Baskes, Prog. Surf. Sci. **79**, 28 (2005)
2. P.J. Hsu, S.K. Lai, J. Chem. Phys. **124**, 44711 (2006)
3. M. Haruta, Nature **437**, 1098 (2005)
4. (a) J. Luo, M.M. Maye, V. Petkov, N.N. Kariuki, L. Wang, P. Njoki, D. Mott, Y. Lin, C.J. Zhong, Chem. Mater. **17**, 3086(2005) (b) Catalysis by Metals and Alloys, V. Ponec and G.C. Bond, (Ed.) Elsevier, 1995
5. C.S. Kim, C. Korzeniewski, Anal. Chem. **69**, 2349 (1997)
6. M.S. Chen, D. Kumar, C.-W. Yi, D.W. Goodman, Science **310**, 291 (2005)
7. C. Mihut, C. Descorme, D. Duprez, M. Amiridis, J. Catal. **212**, 125 (2002)
8. H. Lang, S. Maldonado, K.J. Stevenson, B.D. Chandler, J. Am. Chem. Soc. **126**, 12949 (2004)
9. J. Luo, V.W. Jones, M.M. Maye, L. Han, N.N. Kariuki, C.J. Zhong, J. Am. Chem. Soc. **124**, 13988 (2002)
10. J. Luo, P. Njoki, Y. Lin, L.Wang, D. Mott, C.J. Zhong, Electrochem. Comm. **8**, 581 (2006)
11. J. Luo, P. Njoki, Y. Lin, D. Mott, L. Wang, C.J. Zhong, Langmuir **22**, 2892 (2006)
12. M. Brust, M. Walker, D. Bethell, D.J. Schiffrin, R.J. Whyman, Chem. Soc. Chem. Commun., 1994, 801
13. M.J. Hostetler, C.J. Zhong, B.K.H. Yen, J. Anderegg, S.M. Gross, N.D. Evans, M.D. Porter, R.W. Murray, J. Am. Chem. Soc. **120**, 9396 (1998)
14. D.C. Meier, D.W. Goodman, J. Am. Chem. Soc. **126**, 1892 (2004)
15. J.E. Bailie, G.J. Hutchings, Chem. Commun. **12151**, (1999)
16. M.Ø. Pedersen, S. Helveg, A. Ruban, I. Stensgaard, E. Laegsgaard, J.K. NØrskov, F. Besenbacher, Surf. Sci. **426**, 395 (1999)
17. J.W.A. Sachtler, G.A. Somorjai, J. Catal. **81**, 77 (1983)
18. Q. Ge, C. Song, L.Wang, Comp. Mater. Sci. **35**, 247 (2006)
19. C. Song, Q. Ge, L. Wang, J. Phys. Chem. B **109**, 22341 (2005)